

## Accepted Manuscript

Construction of Heterometallic  $M_2Pd_3$  Supramolecular Cages via a Metalloligand Strategy as Heterogeneous Catalyst for Suzuki–Miyaura Coupling Reaction

Xi-Ren Wu, Su-Yang Yao, Lian-Qiang Wei, Li-Ping Li, Bao-Hui Ye

PII: S0020-1693(18)30771-0  
DOI: <https://doi.org/10.1016/j.ica.2018.07.009>  
Reference: ICA 18355

To appear in: *Inorganica Chimica Acta*

Received Date: 18 May 2018  
Revised Date: 2 July 2018  
Accepted Date: 4 July 2018

Please cite this article as: X-R. Wu, S-Y. Yao, L-Q. Wei, L-P. Li, B-H. Ye, Construction of Heterometallic  $M_2Pd_3$  Supramolecular Cages via a Metalloligand Strategy as Heterogeneous Catalyst for Suzuki–Miyaura Coupling Reaction, *Inorganica Chimica Acta* (2018), doi: <https://doi.org/10.1016/j.ica.2018.07.009>

This is a PDF file of an unedited manuscript that has been accepted for publication. As a service to our customers we are providing this early version of the manuscript. The manuscript will undergo copyediting, typesetting, and review of the resulting proof before it is published in its final form. Please note that during the production process errors may be discovered which could affect the content, and all legal disclaimers that apply to the journal pertain.



**Construction of Heterometallic  $M_2Pd_3$  Supramolecular Cages via a  
Metalloligand Strategy as Heterogeneous Catalyst for Suzuki–Miyaura Coupling  
Reaction**

Xi-Ren Wu,<sup>a,b</sup> Su-Yang Yao,<sup>a</sup> Lian-Qiang Wei,<sup>a</sup> Li-Ping Li,<sup>a</sup> and Bao-Hui Ye<sup>\*a</sup>

<sup>a</sup>*MOE Key Laboratory of Bioinorganic and Synthetic Chemistry, School of Chemistry and Chemical Engineering Sun Yat-sen University, Guangzhou 510275 (P. R. China).  
E-mail: [cesybh@mail.sysu.edu.cn](mailto:cesybh@mail.sysu.edu.cn)*

<sup>b</sup>*School of Pharmacy, Guangdong Medical University, Dongguan, 523808, China*

**ABSTRACT**

On the basis of hard soft acid base theory, two neutral heterometallic  $M_2Pd_3$  supramolecular cages,  $[Al_2Pd_3(L)_6Cl_6]$  (**1**) and  $[Fe_2Pd_3(L)_6Cl_6]$  (**2**) (where HL is 1-(4-(1H-imidazol-1-yl)phenyl)butane-1,3-dione), have been constructed by using the tripodal  $M(L)_3$  as metalloligands in combination with  $PdCl_2$  or  $Pd(MeCN)_2Cl_2$ . The supramolecular cage can be described as a trigonal bipyramid with two  $M^{3+}$  ions occupying at the two axial sites in  $\Delta\Delta$  or  $\Lambda\Lambda$  configurations and three  $Pd^{2+}$  ions sitting in the three equatorial positions with square planar geometry in *trans* configuration. The supramolecular cages exhibit high catalytic activity for the Suzuki–Miyaura coupling with arylbromide or arylchloride and phenylboronic acid in biorenewable solvent glycerol under mild conditions. Moreover, the catalyst can be readily recycled and reused at least five times without loss of catalytic activity. The high catalytic performance may be attributed to the distinct properties of the cage structure with uniformly distributive and well-defined Pd active centres on the cage surfaces. The high stability in the cage structure also prevents Pd leaching out and agglomeration.

**Keywords:** Supramolecular cages; Metalloligand; Palladium complexes; Heterogeneous catalyst; Suzuki–Miyaura coupling.

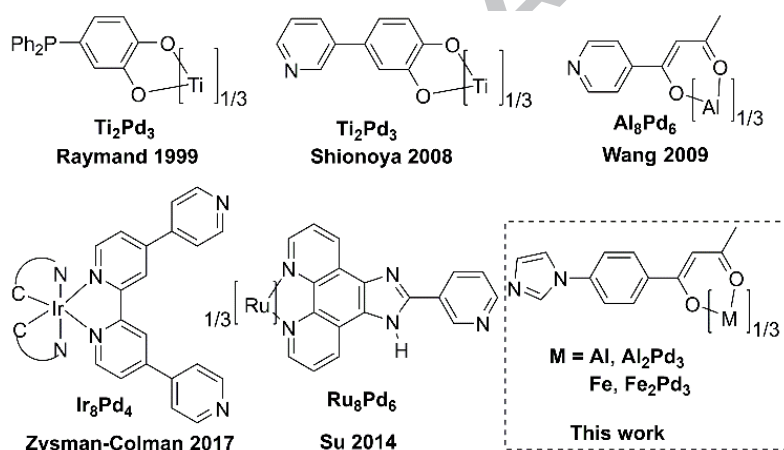
## 1. Introduction

Palladium catalysis carbon-carbon coupling reactions, such as Suzuki–Miyaura, Heck and Sonogashira reactions, have numerous potential applications in synthesis of biologically active compounds and pharmaceuticals.[1-6] However, many of Pd catalysts are limited to homogeneous reactions, in which the catalysts suffer from recovery, leading to the loss of the expensive Pd metal and organic ligands. The use of a heterogeneous catalyst instead provides the possibility to easily separate and recycle the catalyst. Great efforts have been devoted to the preparation of actively recyclable Pd catalysts via immobilization of catalysts on the solid supports, such as magnetic nanoparticles, activated carbon, silica, zeolites, carbon nanotubes, metal oxides, clays, organic polymers and metal-organic frameworks.[7-16] In spite of great advances, the active sites on these solid supports are not always accessible for the reactions and very few achieve uniform distribution as an isolated single-site. In many cases, the catalytic activities are lower than those in the homogeneous counterparts and harsh reaction conditions are always required. Therefore, high efficient, easily separable and reusable catalyst systems are still highly desired.

To overcome these problems, we pay our attention to supramolecular cage that not only arranges the catalytic center in an isolated single-site with a well-defined structure but also maximally exposes the active sites to the substrates to enhance the catalytic activity due to the discrete structure. In fact, many homonuclear Pd supramolecular cages have been assembled,[17-24] and some of them have also been

used as catalysts for carbon-carbon coupling reactions.[25-35] However, heterometallic Pd supramolecular cage is still rare.[36-42] On the basis of hard soft acid base (HSAB) theory, Raymond, Shionoya and Wang have successfully constructed heterometallic Pd supramolecular cages via a metalloligand strategy (Scheme 1).[36-40] But the catalytic activity of these heterometallic Pd complexes has never been exploited. Specifically, the synthesis of heterometallic Pd coordination polymers with the selected metalloligands is a very attractive area concerning the applications as catalysts.[43-46] The synergistic effect between Pd and the other metal ion through the ligand in promotion of catalytic activity has been observed.[47-49] Follow these synthetic strategies, a exotopic bifunctional ligand with N-donor and  $\beta$ -diketone chelating donors at the terminal were employed to construct heterometallic supramolecular cages. Each ligand may bind to two separated metal ions, the chelating nature of  $\beta$ -diketone ensures to bind to a hard metal ion in high stability and a negative charge on each ligand allows access to neutral tripodal metalloligand with a  $M^{3+}$  metal ion. Furthermore, the N-donor may bind to a  $Pd^{2+}$  ion as a potential catalytic center and the vector angle between the N-donor lone pair and the  $\beta$ -diketone chelate in an appropriate angle allows to form a cage structure. The long and rigid rod-like ligand would make sure the supramolecular cages possess big windows that the substrates could readily pass through and the catalytic centers locate in the appropriate sites separately. Such structure feature would help the active component  $PdCl_2$  to promote both the in-cage and out-cage reactions with high efficiency. It can be anticipated that such a rational design will lead to excellent

catalytic activity because the cages allow maximum exposure of the active sites to reactants. Indeed, two heterometallic  $M_2Pd_3$  supramolecular cages  $[Al_2Pd_3(L)_6Cl_6]$  (**1**) and  $[Fe_2Pd_3(L)_6Cl_6]$  (**2**), (where HL = 1-(4-(1H-imidazol-1-yl)phenyl)butane-1,3-dione) were constructed via the metalloligand strategy. The catalytic experiments showed that the  $M_2Pd_3$  cages were highly efficient for the Suzuki–Miyaura cross-coupling reaction in biorenewable solvent glycerol under mild conditions. The catalyst could be recycled at least five times without loss of catalytic activity.



Scheme 1. The diagram of metalloligands for heterometallic supramolecular cages

## 2. Experimental

### 2.1. General procedures

All commercial reagents and solvents were used without further purification. Electrospray ionization mass spectra (ESI-MS) were obtained on a Shimadzu

LCMS-2010A Liquid Chromatography Mass spectrometer. The C, H, and N microanalyses were carried out with a Vario EL elemental analyser.  $^1\text{H}$  NMR spectra were recorded with a Bruker AV 400 spectrometer by using the solvent as an internal standard. Thermogravimetric data were collected on a NETZSCH TG 209 F3 analyser in nitrogen atmosphere at a heating rate of  $10\text{ }^\circ\text{C min}^{-1}$  from ambient temperature to  $850\text{ }^\circ\text{C}$ . Powder X-ray diffraction patterns were recorded on a D8 ADVANCE diffractometer with  $\text{Cu-K}_\alpha$  radiation ( $\lambda = 1.5409\text{ \AA}$ ) at a scanning rate of  $4^\circ\text{ min}^{-1}$  with  $2\theta$  ranging from  $5$  to  $35^\circ$ . Transmission electron microscopy (TEM) images were taken with a FEI Tecnai G2 F20 transmission electron microscope operating at an accelerated voltage of  $200\text{ kV}$ . X-ray photoelectron spectroscopy (XPS) measurements were made on a Thermo Fisher Scientific ESCALAB250 machine with a monochromatic  $\text{Al-K}$  source operated at  $150\text{ W}$  and the pass energy of the analyser was kept at  $10\text{ eV}$ . All the binding energies were calibrated by using the contaminant carbon ( $\text{C1s} = 284.6\text{ eV}$ ) as a reference. Pd elemental analyses were performed by inductively coupled plasma atomic emission spectroscopy (ICP-AES) using a TJA IRIS HR ICP instrument. The ligands HL was prepared according to our previously published procedures.[50]

## 2.2. Syntheses of metalloligands $[\text{Al}(\text{L})_3]$ and $[\text{Fe}(\text{L})_3]$

$\text{M}(\text{NO}_3)_3 \cdot 9\text{H}_2\text{O}$  ( $1\text{ mmol}$ ), HL ( $3.5\text{ mmol}$ ) and  $\text{NaHCO}_3$  ( $3.5\text{ mmol}$ ,  $0.294\text{ g}$ ) were dissolved in  $100\text{ mL}$  of  $\text{MeOH}/\text{H}_2\text{O}$  ( $1:1\text{ v/v}$ ) and stirred until a white or red product precipitated (about  $24\text{ h}$ ). The resultant precipitate was filtered and washed with water.

The crude product was extracted with  $\text{CHCl}_3$  and dried over anhydrous  $\text{MgSO}_4$ . The  $\text{CHCl}_3$  solvent was removed under reduced pressure to afford product as a white or red solid. Yields for  $\text{Al}(\text{L})_3$ , 0.556 g, 78%, MS:  $m/z = 709 [M+H]^+$ ; for  $\text{Fe}(\text{L})_3$ , 0.473 g, 64%, MS:  $m/z = 738 [M+H]^+$ .

### 2.3. Syntheses of heterometallic cages $[\text{Al}_2\text{Pd}_3(\text{L})_6\text{Cl}_6]$ (**1**) and $[\text{Fe}_2\text{Pd}_3(\text{L})_6\text{Cl}_6]$ (**2**)

A mixture of DMSO/ $\text{CH}_2\text{Cl}_2$  solvent (2 mL, v:v = 1:1) was carefully layered over a solution of  $\text{Al}(\text{L})_3$  in  $\text{CH}_2\text{Cl}_2$  (0.01 mmol, 1 mL). Then, a solution of  $\text{PdCl}_2$  in DMSO (0.015 mmol, 2 mL) was layered on the top of the buffer. Yellowish, prism-shaped X-ray quality crystals of **1**·5DMSO·3 $\text{CH}_2\text{Cl}_2$  was obtained after 10 days. The dark-red block crystals of **2**·solvent was obtained via layering a solvent of DMF/MeOH (2 mL, v:v = 1:1) over a solution of  $\text{Pd}(\text{CH}_3\text{CN})_2\text{Cl}_2$  in DMF (1 mL, 0.015 mmol), then, a solution of  $\text{Fe}(\text{L})_3$  in MeOH (1 mL, 0.01 mmol) on the top of the buffer. Crystals **1** and **2** were filtered and washed with DMSO three times, followed by soaking in methanol for two days. Subsequently, solids **1** and **2** were collected via centrifugation and dried at 150 °C under vacuum for 24 h. Yield for **1**·2DMSO, 7.6 mg, 72%, Anal. Calcd for  $\text{C}_{82}\text{H}_{78}\text{Cl}_6\text{Al}_2\text{N}_{12}\text{O}_{14}\text{S}_2\text{Pd}_3$ : C 46.77, H 3.73, N 7.98. Found: C 46.61, H 4.01, N 7.73; for **2**·2DMF, 5.0 mg, 49%, Anal. Calcd for  $\text{C}_{84}\text{H}_{80}\text{Cl}_6\text{Fe}_2\text{N}_{14}\text{O}_{14}\text{Pd}_3$ : C 46.85, H 3.74, N 9.11. Found: C 46.67, H 3.54, N 9.01.

### 2.4. General procedure for the Suzuki-Miyaura coupling reaction

Aryl halide (1.0 mmol), aryl boronic acid (1.1 mmol),  $\text{K}_2\text{CO}_3$  (1.5 mmol) and



catalyst (0.02 mol%) were mixed together in 4.0 mL glycerol and allowed to react at 80 °C for 2 h. After that, the reaction mixture was cooled to room temperature and the organic residue was extracted from glycerol phase by CH<sub>2</sub>Cl<sub>2</sub> (3 × 5 mL). Removal of solvent CH<sub>2</sub>Cl<sub>2</sub>, the crude residue was purified by silica gel chromatography to afford pure product, which was identified using <sup>1</sup>H NMR and <sup>13</sup>C NMR analyses (see ESI).

### 2.5. General procedure for catalyst recovery

Once the reaction was stopped, the organic residues were extracted from glycerol phase by CH<sub>2</sub>Cl<sub>2</sub> (3 × 5 mL). Then, the glycerol phase was maintained under reduced pressure with stirring at 80 °C for 30 min. The fresh substrates were directly added to the recovered glycerol phase in the same tube for the next run reaction under the corresponding conditions.

### 2.6. Crystallographic analysis

The diffraction intensities for **1** and **2** were collected on an Oxford Gemini S Ultra CCD Area detector diffractometer with graphite-monochromated Cu K<sub>α</sub> radiation (λ = 1.54178 Å). All of the data were corrected for absorption effect using the CrysAlisPro software.[51] The structures were solved by direct methods with SHELXT[52] and refined with full-matrix least squares refinements using SHELXL[53] within the Olex2 suite.[54] All non-hydrogen atoms were refined anisotropically. All hydrogen atoms were included in the final structure factor calculation at idealized positions and were allowed to ride on the neighbouring atoms.

The structure of **2** contains accessible voids that are filled in a spot of diffuse electron density belonging to uncoordinated solvent. The SQUEEZE routine of PLATON was used to remove remaining electron density corresponding to solvent not reported in the calculated formula.[55] The crystal data and the details of data collection and refinement for the complexes are summarized in Table 1. The selected bond distances and angles are listed in Table S1 in the Supporting Information.

**Table 1.** Crystallographic data for complexes **1** and **2**.

Complex	1·5DMSO·3CH <sub>2</sub> Cl <sub>2</sub>	2·3DMF·MeCN·H <sub>2</sub> O
Molecular formula	C <sub>91</sub> H <sub>102</sub> Cl <sub>12</sub> Al <sub>2</sub> N <sub>12</sub> O <sub>17</sub> S <sub>5</sub> Pd <sub>3</sub>	C <sub>89</sub> H <sub>93</sub> Cl <sub>6</sub> Fe <sub>2</sub> N <sub>16</sub> O <sub>16</sub> Pd <sub>3</sub>
<i>Mr</i>	2594.71	2286.40
Crystal system	triclinic	triclinic
Space group	<i>P</i> -1	<i>P</i> -1
<i>a</i> [Å]	16.7428(16)	17.1396(4)
<i>b</i> [Å]	18.0798(14)	19.0469(5)
<i>c</i> [Å]	20.8624(16)	19.1412(8)
<i>a</i> [°]	70.613(7)	111.923(3)
<i>β</i> [°]	89.475(7)	101.723(2)
<i>γ</i> [°]	68.511(9)	104.074(2)
<i>V</i> [Å <sup>3</sup> ]	5497.3(9)	5314.4(3)
<i>Z</i>	2	2
<i>D<sub>c</sub></i> (g cm <sup>-3</sup> )	1.568	1.418
<i>μ</i> (mm <sup>-1</sup> )	8.195	8.070
Data collected	17020	16972
Observed reflections	13619	12886
<sup>a</sup> <i>R</i> <sub>1</sub> [I > 2σ(I)]	0.0609	0.0717
<sup>b</sup> <i>wR</i> <sub>2</sub> (F <sup>2</sup> ) [I > 2σ(I)]	0.1762	0.1850
GOF on F <sup>2</sup>	1.029	1.010

$$^a R_1 = \sum ||F_o| - |F_c|| / \sum |F_o|, \quad ^b wR = [\sum w(F_o^2 - F_c^2)^2 / \sum w(F_o^2)^2]^{1/2}$$

CCDC-1586307 and 15866312 contain the crystallographic information for this paper. All these data can be obtained free of charge from the Cambridge Crystallographic Data Centre via [www.ccdc.cam.ac.uk/data\\_requests/cif](http://www.ccdc.cam.ac.uk/data_requests/cif).

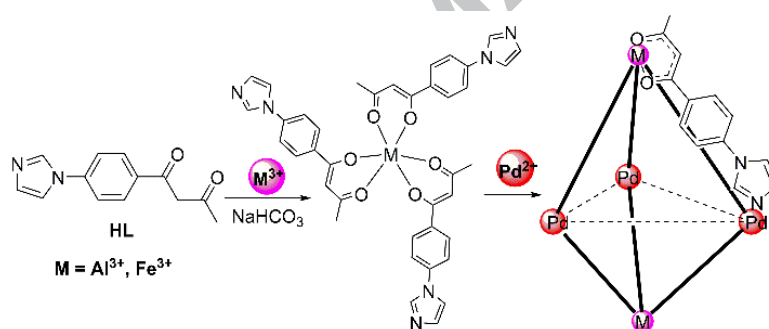
### 3. Results and Discussion

#### 3.1. Ligand Design and Synthesis of Complexes via a Metalloligand Strategy

The bifunctional ligand HL containing a terminal N-donor imidazole group and a  $\beta$ -diketone chelate linking via a phenyl spacer was successfully synthesized by Claisen condensation of N-donor substituted acetophenone and ethyl acetate.[50] It can be seen as three potential exotopic donors with distinctly coordinated feature binding to two different metal ions, the chelating nature of  $\beta$ -diketone is hard with negative charge and favors a hard  $M^{3+}$  metal ion to form a neutral octahedral geometry. On the other hand, the N-donor ligand is relative soft and bind to a Pd ion as a potential catalytic center. A ligand containing dual these functional groups arranged in a proper geometry can generate a cage structure. The introduction of phenyl ring between the N-donor and  $\beta$ -diketone as a space allows the potential catalytic centers separately.

Though hard metal ions can exclusively bind at the  $\beta$ -diketone site, softer metal centers such as  $Pd^{2+}$  and  $Zn^{2+}$  may not discriminate sufficiently between the  $\beta$ -diketone and N-donor coordination modes. Thus,  $Zn^{2+}$  or  $Pd^{2+}$  reacted with HL like ligand, resulting in a product containing indiscriminate N-donor and  $\beta$ -diketone coordination to  $Zn^{2+}$  or  $Pd^{2+}$  ions.[50, 56-58] Here, we opted to synthesize  $\beta$ -diketone-hard metal complex first as a metalloligand (see Scheme 2).[36-40, 59-62] Indeed, when the ligand reacted with  $M(NO_3)_3$  ( $M = Al^{3+}$  or  $Fe^{3+}$ ) in a 3:1 ratio in the

presence of  $\text{NaHCO}_3$  as a base, a neutral metalloligand  $\text{M}(\text{L})_3$  was afford as a white or red powder. Each of the tripodal  $\text{M}(\text{L})_3$  metalloligand with three N-donors can coordinate to three  $\text{Pd}^{2+}$  ions, leading to a heterometallic supramolecular complex, in which each  $\text{Pd}^{2+}$  ion may be further coordinated by two labile chlorides to meet charge balance and coordination saturation. It should be pointed out that the introduction of labile ligand such as chloride will be benefit for catalysis. Neutral complex **1** was prepared by layering a solution of  $\text{PdCl}_2$  in DMSO over a solution of  $\text{Al}(\text{L})_3$  in  $\text{CH}_2\text{Cl}_2$ . While complex **2** was obtained by layering a solution of  $\text{Fe}(\text{L})_3$  in MeOH over a solution of  $\text{Pd}(\text{MeCN})_2\text{Cl}_2$  in DMF.



Scheme 2. Synthesis of heterometallic  $\text{M}_2\text{Pd}_3$  supramolecular cages via the metalloligand strategy.

Complexes **1** and **2** are not soluble in common solvents such as MeOH,  $\text{CHCl}_3$  and DMF. Due the crystals easy effloresce under atmosphere, the lower boiling point solvent molecules are tried to be removed by drying at  $150\text{ }^\circ\text{C}$  under vacuum for 24 h before analysis. Elemental analyses and thermogravimetric analysis (TGA, see Figures S1 and S2) were used to determine the number of the solvent molecules. It was found that there were two DMSO and two DMF molecules in complexes **1**. 2DMSO (7.41%

in theory vs 7.75% in experiment) and **2**·2DMF (6.80% in theory vs 7.20% in experiment), respectively, from the TGA curves.

### 3.2. Structural Analysis and Characterization

In order to observe the structure of the heterometallic supramolecular cage, single crystal structures of **1**·5DMSO·3CH<sub>2</sub>Cl<sub>2</sub> and **2**·3DMF·MeCN·H<sub>2</sub>O were measured by X-ray crystallography, respectively. They crystallize in the *P*-1 space group. The heterometallic supramolecular cages are indeed confirmed as shown in Figure 1. Each cage consists of two homochiral M(L)<sub>3</sub> fragments in  $\Delta\Delta$  or  $\Lambda\Lambda$  configurations that are linked by three PdCl<sub>2</sub> units. Thus each cage molecule is chiral, indicating that the homochiral assembly between M(L)<sub>3</sub> metalloligands occurs during the course of reaction with Pd<sup>2+</sup>. The similar case was also observed in [Al<sub>2</sub>Zn<sub>3</sub>Br<sub>6</sub>(L1)<sub>6</sub>] (L1 is 1-(4-pyridyl)butane-1,3-dione) cage,[40] but a mesocate was reported in [Ti<sub>2</sub>Pd<sub>3</sub>Br<sub>6</sub>(L2)<sub>6</sub>]<sup>4+</sup> (L2 is 4-PPh<sub>2</sub>-catechol) cage,[36, 37] this may relate to the ligand structure. However, there are a pair of enantiomeric molecules ( $\Delta\Delta$  and  $\Lambda\Lambda$ ) in each unit cell, they are racemate and crystallize in achirality. The M<sub>2</sub>Pd<sub>3</sub> heterometallic supramolecular cage may be described as a trigonal bipyramid, two M<sup>3+</sup> cations situate at the axial corners with a M···M distance of 19.71 Å for **1** and 20.11 Å for **2** and three Pd<sup>2+</sup> cations locate in the equatorial plane with a Pd···Pd distance of 9.99-11.04 Å for **1** and 9.78-10.43 Å for **2**. The M···Pd distances are in the rang 11.43-11.75 Å and 11.47-11.98 Å for **1** and **2**, respectively. These much enlongate the

distances between  $\text{Pd}^{2+}$  ions and form larger rhombic windows, comparison with those of the reported heterometallic cages  $[\text{Al}_2\text{Zn}_3\text{Br}_6(\text{L1})_6]$  ( $\text{Al}\cdots\text{Al} = 11.26 \text{ \AA}$ )[40] and  $[\text{Ti}_2\text{Pd}_3\text{Br}_6(\text{L2})_6]^{4+}$  ( $\text{Ti}\cdots\text{Ti} = 6.76 \text{ \AA}$ ).[36, 37] Each  $\text{M}^{3+}$  ion is triply chelated by the  $\beta$ -diketonate moieties of L ligand in a slightly distorted octahedral geometry with the *fac* configuration, indicating that an isomerization process (from *mer* to *fac*) may occurs during the course of assembly to form cage structure. The Al–O and Fe–O distances are in the range 1.860(5)–1.893(5)  $\text{\AA}$  and 1.968(6)–2.017(6)  $\text{\AA}$ , respectively, which are consistent with the reports.[40] Each of  $\text{Pd}^{2+}$  cation is coordinated by two N-donors from the imidazolate of L ligand and two chloride anions in a square planar with a *trans* configuration ( $\angle\text{Cl-Pd-Cl} = 174\text{--}179^\circ$ ,  $\angle\text{N-Pd-N} = 174\text{--}178^\circ$ ). The bond distances of Pd–N and Pd–Cl are in the range of 1.998(5)–2.015(6)  $\text{\AA}$  and 2.2896(17)–2.3141(19)  $\text{\AA}$  for **1**, and 1.994(7)–2.024(6)  $\text{\AA}$  and 2.282(2)–2.299(3)  $\text{\AA}$  for **2**, respectively.

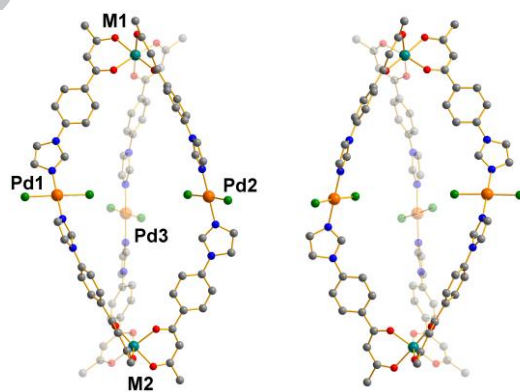


**Figure1.** Crystal structures of homochiral heterometallic  $[\text{M}_2\text{Pd}_3(\text{L})_6\text{Cl}_6]$  supramolecular cages  $\Lambda\Lambda$  (left) and  $\Delta\Delta$  (right). H-atoms and solvents are omitted for clarity. Color code: gray, C; blue, N; red, O; green, Cl; orange, Pd; teal, M (Al, Fe). Selected bond distances ( $\text{\AA}$ ) and angles ( $^\circ$ ) for **1** and **2** (in parentheses):  $\text{M1}\cdots\text{Pd1} = 11.655(2)$  (11.569(5)),  $\text{M1}\cdots\text{Pd2} = 11.605(2)$  (11.556(4)),  $\text{M1}\cdots\text{Pd3} = 11.458(2)$  (11.840(3)),  $\text{M2}\cdots\text{Pd1} = 11.494(2)$  (11.581(3)),  $\text{M2}\cdots\text{Pd2} = 11.434(2)$  (11.473(4)),  $\text{M2}\cdots\text{Pd3} = 11.759(2)$  (11.982(6)),  $\text{Pd1}\cdots\text{Pd2} = 9.999(1)$  (10.354(2)),  $\text{Pd1}\cdots\text{Pd3} = 10.332(1)$  (9.787(4)),  $\text{Pd2}\cdots\text{Pd3} = 11.044(1)$  (10.429(3)) and  $\text{M1}\cdots\text{M2} = 19.713(2)$  (20.110(2));

$\angle \text{Pd1-M1-Pd3} = 58.1(1) (49.4(1))$ ,  $\angle \text{Pd1-M1-Pd2} = 50.9(2) (53.2(2))$ ,  $\angle \text{Pd2-M1-Pd3} = 57.2(1) (52.9(2))$ ,  $\angle \text{Pd1-M2-Pd3} = 52.8(1) (49.1(2))$ ,  $\angle \text{Pd1-M2-Pd2} = 51.7(2) (53.4(2))$ ,  $\angle \text{Pd2-M2-Pd3} = 56.8(1) (52.8(2))$ ,  $\angle \text{Cl-Pd1-Cl} = 175.5(1) (178.1(1))$ ,  $\angle \text{N-Pd1-N} = 177.3(1) (178.1(2))$ ,  $\angle \text{Cl-Pd2-Cl} = 178.7(2) (174.6(2))$ ,  $\angle \text{N-Pd2-N} = 174.2(1) (178.4(1))$ ,  $\angle \text{Cl-Pd3-Cl} = 179.0(1) (178.5(2))$  and  $\angle \text{N-Pd3-N} = 174.6(1) (177.7(1))$ .

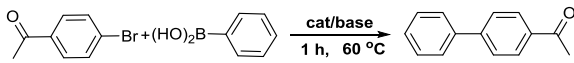
The powder X-ray diffraction (PXRD) of complexes **1** and **2** were also collected, respectively (see Figure S3). The discrepancies in PXRD patterns based on the stimulation from single-crystal structures and the as-synthesized samples remain, these might result from preferred crystallite orientation and anisotropic particle broadening. TGA of the as-synthesized samples showed that they lost solvent molecules as the temperature was elevated. Complex **1** decomposed when the temperature reached about 250 °C, and **2** at about 290 °C, indicating that they have good thermal stability.

### 3.3. Catalysis for the Suzuki-Miyaura Coupling Reaction

To evaluate the catalytic activity of the synthetic catalysts, 4-bromoacetophenone and phenylboronic acid were used as model compounds for the Suzuki–Miyaura cross coupling reaction in the presence of **1** (0.05 mol%) as a catalyst and  $\text{K}_2\text{CO}_3$  as a base in  $\text{H}_2\text{O}$  under ambient atmosphere at 60 °C for 1 h (Table 2, entry 1). However, the yield was found only in 14%. To our delight, when EtOH was used as a solvent, the monitor experiment revealed that the halide substrate was completely converted into target product (entry 2), indicating that complex **1** is an efficient catalyst for the Suzuki–Miyaura coupling. We also found that catalyst **1** is high activity for the Suzuki–Miyaura coupling in the mixture solvent of EtOH and water (entry 3-5).

However, the catalyst turned from pale yellow to grey black, indicating  $\text{Pd}^{2+}$  ion may be leached out in some degree during the reaction. That is unfavorable to recycle and reuse the catalyst. From the view of green chemistry, the eco-friendly and biorenewable solvents, such as water, ethanol and glycerol, are welcome.[63] When biorenewable solvent glycerol was used instead of EtOH, the target product was afforded in 46%, but increase to 99% at 80 °C. Importantly, catalyst **1** maintained pale yellow initial color after reaction. Base has been regarded as a significant factor in the Suzuki–Miyaura coupling, thus, we turned our attention to test the impact of base (entry 7-12). The experiments revealed that  $\text{K}_2\text{CO}_3$  is the best one.  $\text{Na}_2\text{CO}_3$  has a similar effect and is superior to other bases, such as KOH, NaOH,  $\text{K}_3\text{PO}_4$  and  $\text{NaHCO}_3$ . Moreover, low catalyst loading tests were performed in order to find out the efficiency of the catalyst. We found that the conversion of the reaction would be completed in 2 h in the presence of 0.02 mol% catalyst **1**, but the yield was decreased to 84% when 0.01 mol% **1** was used in 4 h.

**Table 2.** Optimization of the Suzuki-Miyauracoupling conditions under ambient atmosphere <sup>a</sup>

				
Entry	Catalyst	Solvent	Base	Yield (%) <sup>b</sup>
1	1	H <sub>2</sub> O	K <sub>2</sub> CO <sub>3</sub>	14
2	1	EtOH	K <sub>2</sub> CO <sub>3</sub>	99
3	1	EtOH/H <sub>2</sub> O(1:1)	K <sub>2</sub> CO <sub>3</sub>	94
4	1	EtOH/H <sub>2</sub> O(2:3)	K <sub>2</sub> CO <sub>3</sub>	90
5	1	EtOH/H <sub>2</sub> O(3:2)	K <sub>2</sub> CO <sub>3</sub>	99
6	1	glycerol	K <sub>2</sub> CO <sub>3</sub>	46
7	1	glycerol	K <sub>2</sub> CO <sub>3</sub>	99 <sup>c</sup>
8	1	glycerol	Na <sub>2</sub> CO <sub>3</sub>	96 <sup>c</sup>
9	1	glycerol	NaHCO <sub>3</sub>	61 <sup>c</sup>
10	1	glycerol	K <sub>3</sub> PO <sub>4</sub>	55 <sup>c</sup>
11	1	glycerol	KOH	15 <sup>c</sup>
12	1	glycerol	NaOH	19 <sup>c</sup>
13	1	glycerol	K <sub>2</sub> CO <sub>3</sub>	91 <sup>c,a</sup>
14	1	glycerol	K <sub>2</sub> CO <sub>3</sub>	99 <sup>a,e</sup>
15	1	glycerol	K <sub>2</sub> CO <sub>3</sub>	84 <sup>f</sup>



16	2	glycerol	K <sub>2</sub> CO <sub>3</sub>	99 <sup>a,c</sup>
17	2	glycerol	K <sub>2</sub> CO <sub>3</sub>	82 <sup>f</sup>
18	PdCl <sub>2</sub>	glycerol	K <sub>2</sub> CO <sub>3</sub>	<5 <sup>e</sup>
19	PdCl <sub>2</sub> +HL	glycerol	K <sub>2</sub> CO <sub>3</sub>	83 <sup>e</sup>

<sup>a</sup> Reaction conditions: 4-bromoacetophenone (1.0 mmol), phenylboronic acid (1.1 mmol), catalyst (0.05 mol%), and base (1.5 mmol) in solvent (4.0 mL) under ambient atmosphere at 60 °C for 1 h. <sup>b</sup>Yield was determined by <sup>1</sup>HNMR with mesitylene as internal standard. <sup>c</sup>80 °C, 1h. <sup>d</sup>catalyst 0.02 mol%. <sup>e</sup>80 °C, 2 h. <sup>f</sup>catalyst 0.01 mol%, 80 °C, 4 h.

The catalytic activity of catalyst **2** was also evaluated under the optimal conditions (entries 16 and 17). The yield is 99% in the identical conditions, indicating that catalysts **1** and **2** have excellent catalytic activity for the Suzuki-Miyaura coupling under the reaction conditions. These may be attributed to the stronger electron-rich effect of imidazolyl group in HL ligand, which favors both the oxidative addition and reductive elimination steps in the catalytic cycle.[25, 64-66] Moreover, the control experiments were also performed. When PdCl<sub>2</sub> was employed as a catalyst, only a little product was found. The addition of ligand HL to the above reaction solution, the yield markedly increased to 83% under the reaction conditions, but the catalyst turned to black at the end of reaction and hard to be reused, indicating that the formation of heterometallic cage benefits to increase the stability of catalyst and catalytic activity.

With the optimized reaction conditions in hand, the scopes and limitations of the catalytic reaction were examined. Under the optimal conditions, a variety of substitutions of electron-withdrawing such as COCH<sub>3</sub>, CHO, CN, and NO<sub>2</sub> groups on arylbromide completely converted into the corresponding target products in yield of 99% (Table 3, entry 1-4). These functional groups would be readily used as sources for further derivations. Moreover, the reaction activity of the electron-neutral substrate bromobenzene is slightly inferior, affording in 83% yield, but increase to 99%

via extension the reaction time to 4 h. For more challenging electron-donating aryl bromides, with the exception of ortho-methyl aryl bromide (15%), the yields were good in 86–96% (entry 6-9) when the temperature was set at 90 °C for 4 h. The lower yield of the ortho-substituent demonstrated that steric effect of the aryl bromide was sensitive to the reaction. In addition, reactions using other aryl boronic acids (entry 10-14) were also performed, and the corresponding biaryl products were obtained in good to excellent yields, regardless of electron-deficient and electron-rich phenylboronic acid, suggesting the electronic character of the substituents has minimal impact on the reaction. Finally, a dual Suzuki-Miyaura coupling formation of a polyaromatic compound in one-pot was also performed under the optimal conditions. 1,4-dibromobenzene reacted with phenylboronic acid efficiently, affording the target product p-terphenyl in yield of 99% in 4 h (entry 15). No monocoupling product was observed.

Encouraged by the high activity of the catalyst **1**, the coupling reactions of aryl chlorides with phenylboronic acid were observed (entry 16-21), which is much more difficult than aryl bromide because of the larger bond energy of C-Cl bond, and harsher reaction conditions are required. To our delight, the activated aryl chlorides with electron-withdrawing groups gave 98-99% yield in the presence of 0.1% catalyst **1** at 110 °C, whereas an inactivated one gave 66-90% yield. Unfortunately, only trace product was obtained for the strong electron-rich aryl chloride (entry 21).

These results demonstrate the broad substrate scope and high catalytic efficiency of catalyst **1** for the Suzuki-Miyaura coupling reaction. The highly catalytic activity of

the catalyst **1** may be attributed to the distinct cage structure with rigid geometry that allows the catalytic center in a single site and maximum exposure to substrates. Notably, the catalytic reactions are under mild conditions, not requiring the exclusion of air and water.

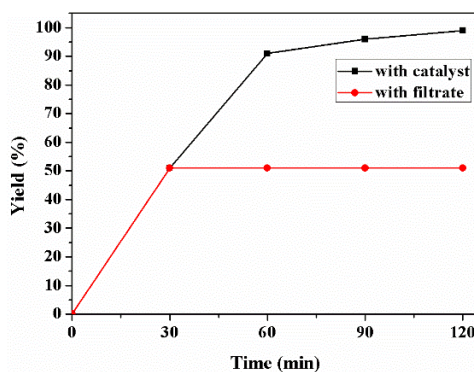
Table 3. The Suzuki-Miyaura coupling catalysed by **1**.

$\text{R}^1\text{-C}_6\text{H}_4\text{-X} + \text{HO}_2\text{B-C}_6\text{H}_4\text{-R}^2 \xrightarrow[\text{2 h, 80 }^\circ\text{C}]{\text{cata 1 (0.02 mol\%), glycerol, K}_2\text{CO}_3} \text{R}^1\text{-C}_6\text{H}_4\text{-C}_6\text{H}_4\text{-R}^2$				
Entry	Arylhalide	R <sup>2</sup>	Product	Yield (%) <sup>a</sup>
1		H		99
2		H		99
3		H		99
4		H		99
5		H		83, 99 <sup>c</sup>
6		H		81 <sup>c</sup> , 96 <sup>d</sup>
7		H		90 <sup>d</sup>
8		H		15 <sup>d</sup>
9		H		86 <sup>d</sup>
10		F		99 <sup>c</sup>
11		CH <sub>3</sub>		99 <sup>c</sup>
12		CHO		99 <sup>c</sup>
13		COCH <sub>3</sub>		99 <sup>c</sup>
14		OCH <sub>3</sub>		99 <sup>c</sup>
15		H		99 <sup>c,e</sup>
16		H		59 <sup>d</sup> , 99 <sup>f</sup>
17		H		99 <sup>f</sup>
18		H		98 <sup>f</sup>
19		H		90 <sup>f</sup>
20		H		66 <sup>f</sup>
21		H		5 <sup>f</sup>

<sup>a</sup> Reaction conditions: aryl halide (1.0 mmol), aryl boronic acid (1.1 mmol), catalyst **1** (0.02 mol%), and K<sub>2</sub>CO<sub>3</sub> (1.5 mmol) in glycerol (4.0 mL) under ambient atmosphere at 80 °C for 2 h. <sup>b</sup> Yield was determined by <sup>1</sup>HNMR with mesitylene as internal standard. <sup>c</sup> 80 °C, 4 h. <sup>d</sup> 90 °C, 4 h. <sup>e</sup> Phenylboronic acid 2.2 mmol, 3.0 equiv K<sub>2</sub>CO<sub>3</sub>. <sup>f</sup> catalyst 0.1 mol%, 110 °C, 4 h.

### 3.4. Heterogeneity Test and Catalyst Reuse

Leaching of Pd from the catalyst is a vital topic in coupling reaction in heterogeneous reaction. To verify this matter, a hot filtration test was performed.[67] When the coupling reaction of 4-bromoacetophenone and phenyl boronic acid was triggered under the optimal conditions in about 30 min (ca. 51% conversion determined by  $^1\text{H}$  NMR), the liquid phase was collected by hot filtration at the reaction temperature to remove the catalyst. Then, 1.5 equiv of  $\text{K}_2\text{CO}_3$  was added to the filtrate, and the mixture was stirred for another 1.5 h at the reaction temperature. After that,  $^1\text{H}$  NMR analysis of the reaction solution indicated that no further cross-coupling occurred (see Figure 2), demonstrating that catalyst **1** has a good heterogeneous nature and no active species leached into the liquid phase under the reaction conditions. In addition, ICP-AES analysis showed that no detectable palladium was observed in the filtrate after reaction. These results simply that the Pd is

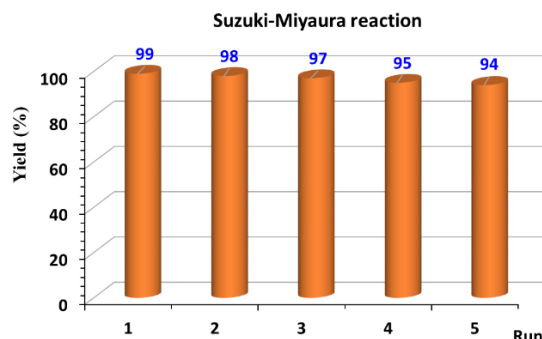


not leached out from the supramolecular cage **1** during the reaction because of the strong interaction between Pd(II) ion and ligand via coordination bonds and catalyst **1** seems to catalyze the coupling in a truly heterogeneous manner.

**Figure 2.** Time conversion plot for the Suzuki-Miyaura reaction conditions (Table 3, entry 1). One of the reactions (black) was carried out in the presence of catalyst **1**, for the other (red), catalyst **1** was filtered and the reaction mixture was allowed to continue the reaction.

The recovery and reuse of a heterogeneous catalyst are of great importance from the views of industry, economy and green chemistry. Therefore, tests of the recyclability of catalyst **1** were carried out using the model reactions, 4-bromoacetophenone and phenylboronic acid under the optimal conditions. After each cycle, the final product was extracted with dichloromethane several times and analysed by  $^1\text{H}$  NMR. As depicted in Figure 3, the recovered catalyst **1** was subsequently used in at least five successive cycles without loss of catalytic activity. PXRD pattern of the reused catalyst **1** showed that the structural integrity of the framework was mostly maintained (see Figure 4), indicating that the supramolecular cages are robust and stable under the reaction conditions. To observe the state of Pd after catalytic reaction, XPS analysis was performed for the recovered catalyst **1** after the first and the fifth run of the Suzuki–Miyaura coupling reactions. They both exhibit a Pd  $3d_{5/2}$  band at 338 eV and a Pd  $3d_{3/2}$  band at 343 eV, respectively, which are characteristic of  $\text{Pd}^{2+}$ . [68] The weak peaks at 335 and 341 eV are ascribed to the Pd(0)  $3d_{5/2}$  and  $3d_{3/2}$ , respectively (see Figure S4). [69] Meanwhile, transmission electron microscopy (TEM) images of the recycled catalyst **1** also showed that a spot of Pd(0) particles in situ generation during the coupling reaction were uniformly dispersed on the surface of the supramolecular cages and no aggregation Pd(0) nanoparticles were observed (see Figure S5). Therefore, the catalyst is still highly efficient and can be reused.

On the basis of the aforementioned studies, a plausible mechanism is suggested. In the coupling reaction, the  $\text{Pd}^{2+}$  in catalyst **1** seems to undergo a reversible process, in



which  $\text{Pd}^{2+}$  is reduced to  $\text{Pd}(0)$  and immediately oxidized back to the initial  $\text{Pd}^{2+}$  state in situ after the catalytic cycle under the air atmosphere. The distinct coordination and stable structure in supramolecular cage of catalyst **1** plays a key role to reserve the chemical microenvironment of the  $\text{Pd}^{2+}$  center sites, not only isolating  $\text{Pd}^{2+}$  in a single site, but also preventing the agglomeration of active  $\text{Pd}(0)$  species into Pd black.

**Figure 3.** Durability test of catalyst **1** in the Suzuki-Miyaura reaction of 4-bromoacetophenone and phenylboronic acid under the optimal

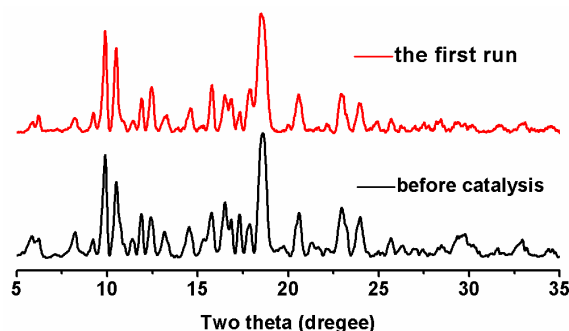


**Figure 4.** PXRD patterns of the as-synthesized sample of **1** and the recovery catalyst **1**.

## Conclusions

In summary, neutral heterometallic  $M_2Pd_3$  supramolecular cages with a trigonal bipyramid geometry have been successfully assembled via metalloligand strategy on the basis of HSAB theory. Homochiral assembly and isomerization of the tripodal  $M(L)_3$  metalloligands occurred during the course of assembly with  $Pd^{2+}$ . The molecular cages exhibit high catalytic activity for the Suzuki–Miyaura coupling reaction under mild conditions and can be readily recycled and reused at least five times without loss of catalytic activity. The excellent catalytic activity can be attributed to the distinct properties of the cage structure in uniformly distributive and well-defined Pd active centers on the cage surfaces. This finding would provide a complementary strategy on design and synthesis of new catalyst for heterogeneous reaction.

## Acknowledgements

This work was supported by the National Natural Science Foundation of China (grant no. 21272284 and 21571195).

## References

- [1] A. Suzuki, *Angewandte chemie international edition*, 50 (2011) 6722-6737.
- [2] R. Martin, S.L. Buchwald, *Accounts Chem Res*, 41 (2008) 1461-1473.

- [3] D. Alberico, M.E. Scott, M. Lautens, *Chem Rev*, 107 (2007) 174-238.
- [4] A. Chatterjee, T.R. Ward, *Catal Lett*, 146 (2016) 820-840.
- [5] J. Le Bras, J. Muzart, *Chem Rev*, 111 (2011) 1170-1214.
- [6] R. Chinchilla, C. Nájera, *Chem Soc Rev*, 40 (2011) 5084-5121.
- [7] S. Ikegami, H. Hamamoto, *Chem Rev*, 109 (2009) 583-593.
- [8] V. Polshettiwar, C. Len, A. Fihri, *Coord Chem Rev*, 253 (2009) 2599-2626.
- [9] M.J. Climent, A. Corma, S. Iborra, *Chem Rev*, 111 (2010) 1072-1133.
- [10] A.r.d. Molnár, *Chem Rev*, 111 (2011) 2251-2320.
- [11] A. Fihri, M. Bouhrara, B. Nekoueishahraki, J.-M. Basset, V. Polshettiwar, *Chem Soc Rev*, 40 (2011) 5181-5203.
- [12] K. Bester, A. Bukowska, W. Bukowski, *Applied Catalysis A: General*, 443 (2012) 181-190.
- [13] M. Yoon, R. Srirambalaji, K. Kim, *Chem Rev*, 112 (2011) 1196-1231.
- [14] J. Liu, L. Chen, H. Cui, J. Zhang, L. Zhang, C.-Y. Su, *Chem Soc Rev*, 43 (2014) 6011-6061.
- [15] M. Zhao, S. Ou, C.-D. Wu, *Accounts Chem Res*, 47 (2014) 1199-1207.
- [16] P. Das, W. Linert, *Coord Chem Rev*, 311 (2016) 1-23.
- [17] M. Fujita, D. Oguro, M. Miyazawa, H. Oka, K. Yamaguchi, K. Ogura, *Nature*, 378 (1995) 469.
- [18] A. Schmidt, A. Casini, F.E. Kühn, *Coord Chem Rev*, 275 (2014) 19-36.
- [19] M. Raynal, P. Ballester, A. Vidal-Ferran, P.W. van Leeuwen, *Chem Soc Rev*, 43 (2014) 1660-1733.
- [20] T.R. Cook, P.J. Stang, *Chem Rev*, 115 (2015) 7001-7045.



- [21] Y.-Y. Zhang, W.-X. Gao, L. Lin, G.-X. Jin, *Coordination Chemistry Reviews*, 344 (2017) 323-344.
- [22] N. Sinha, F.E. Hahn, *Accounts of Chemical Research*, 50 (2017) 2167-2184.
- [23] G.H. Clever, P. Punt, *Accounts of Chemical Research*, 50 (2017) 2233-2243.
- [24] R.A.S. Vasdev, D. Preston, J.D. Crowley, *Chem-Asian J*, 12 (2017) 2513-2523.
- [25] S. Pal, W.-S. Hwang, I.J. Lin, C.-S. Lee, *Journal of Molecular Catalysis A: Chemical*, 269 (2007) 197-203.
- [26] A. John, M.M. Shaikh, R.J. Butcher, P. Ghosh, *Dalton T*, 39 (2010) 7353-7363.
- [27] Q. Zhang, L. He, J.-M. Liu, W. Wang, J. Zhang, C.-Y. Su, *Dalton T*, 39 (2010) 11171-11179.
- [28] D. Samanta, S. Mukherjee, Y.P. Patil, P.S. Mukherjee, *Chem-Eur J*, 18 (2012) 12322-12329.
- [29] D. Samanta, P.S. Mukherjee, *Chem Commun*, 49 (2013) 4307-4309.
- [30] P. Howlader, P.S. Mukherjee, *Chem Sci*, 7 (2016) 5893-5899.
- [31] C.-W. Zhao, J.-P. Ma, Q.-K. Liu, Y. Yu, P. Wang, Y.-A. Li, K. Wang, Y.-B. Dong, *Green Chem*, 15 (2013) 3150-3154.
- [32] T.H. Noh, W. Hong, H. Lee, O.-S. Jung, *Dalton T*, 44 (2015) 787-794.
- [33] S. Pradhan, R.P. John, *New J Chem*, 39 (2015) 5759-5766.
- [34] S. Pradhan, S. Dutta, R.P. John, *New J Chem*, 40 (2016) 7140-7147.
- [35] S. Pradhan, R.P. John, *Rsc Adv*, 6 (2016) 12453-12460.
- [36] X. Sun, D.W. Johnson, D.L. Caulder, R.E. Powers, K.N. Raymond, E.H. Wong, *Angewandte Chemie International Edition*, 38 (1999) 1303-1307.
- [37] X. Sun, D.W. Johnson, D.L. Caulder, K.N. Raymond, E.H. Wong, *J Am Chem Soc*, 123

(2001) 2752-2763.

[38] S. Hiraoka, Y. Sakata, M. Shionoya, *J Am Chem Soc*, 130 (2008) 10058-10059.

[39] Y. Sakata, S. Hiraoka, M. Shionoya, *Chem-Eur J*, 16 (2010) 3318-3325.

[40] H.B. Wu, Q.M. Wang, *Angewandte Chemie*, 121 (2009) 7479-7481.

[41] K. Li, L.-Y. Zhang, C. Yan, S.-C. Wei, M. Pan, L. Zhang, C.-Y. Su, *J Am Chem Soc*, 136 (2014) 4456-4459.

[42] K. Wu, K. Li, Y.-J. Hou, M. Pan, L.-Y. Zhang, L. Chen, C.-Y. Su, *Nat Commun*, 7 (2016) 10487.

[43] Y. Miyazaki, Y. Kataoka, T. Kawamoto, W. Mori, *Eur J Inorg Chem*, 2012 (2012) 807-812.

[44] S.-L. Huang, A.-Q. Jia, G.-X. Jin, *Chem Commun*, 49 (2013) 2403-2405.

[45] X. Li, R. Van Zeeland, R.V. Maligal-Ganesh, Y. Pei, G. Power, L. Stanley, W. Huang, *Acs Catal*, 6 (2016) 6324-6328.

[46] Y. Dong, Y. Li, Y.-L. Wei, J.-C. Wang, J.-P. Ma, J. Ji, B.-J. Yao, Y.-B. Dong, *Chem Commun*, 52 (2016) 10505-10508.

[47] J. Huang, W. Wang, H. Li, *Acs Catal*, 3 (2013) 1526-1536.

[48] L.-X. You, H.-J. Liu, L.-X. Cui, F. Ding, G. Xiong, S.-J. Wang, B.-Y. Ren, I. Dragutan, V. Dragutan, Y.-G. Sun, *Dalton T*, 45 (2016) 18455-18458.

[49] L. You, W. Zong, G. Xiong, F. Ding, S. Wang, B. Ren, I. Dragutan, V. Dragutan, Y. Sun, *Applied Catalysis A: General*, 511 (2016) 1-10.

[50] P. Yang, J.-J. Wu, H.-Y. Zhou, B.-H. Ye, *Cryst Growth Des*, 12 (2011) 99-108.

[51] D. Das, S. Das, P. Singha, K. Malik, A.K. Deb, A. Bhattacharyya, V.A. Kulbachinskii, R. Basu, S. Dhara, S. Bandyopadhyay, A. Banerjee, *Phys Rev B*, 96 (2017).

- [52] G.M. Sheldrick, *Acta Crystallographica Section A: Foundations of Crystallography*, 64 (2008) 112-122.
- [53] G.M. Sheldrick, *Acta Crystallographica Section C: Structural Chemistry*, 71 (2015) 3-8.
- [54] O.V. Dolomanov, L.J. Bourhis, R.J. Gildea, J.A. Howard, H. Puschmann, *J Appl Crystallogr*, 42 (2009) 339-341.
- [55] A. Spek, *J Appl Crystallogr*, 36 (2003) 7-13.
- [56] G.-G. Hou, Y. Liu, Q.-K. Liu, J.-P. Ma, Y.-B. Dong, *Chem Commun*, 47 (2011) 10731-10733.
- [57] B.L. Chen, F.R. Fronczek, A.W. Maverick, *Chem Commun*, (2003) 2166-2167.
- [58] A. Walczak, A.R. Stefankiewicz, *Inorg Chem*, 57 (2018) 471-477.
- [59] B. Chen, F.R. Fronczek, A.W. Maverick, *Inorg Chem*, 43 (2004) 8209-8211.
- [60] Y. Zhang, B. Chen, F.R. Fronczek, A.W. Maverick, *Inorg Chem*, 47 (2008) 4433-4435.
- [61] V.D. Vreshch, A.B. Lysenko, A.N. Chernega, J.A. Howard, H. Krautscheid, J. Sieler, K.V. Domasevitch, *Dalton T*, (2004) 2899-2903.
- [62] L. Carlucci, G. Ciani, S. Maggini, D.M. Proserpio, M. Visconti, *Chem-Eur J*, 16 (2010) 12328-12341.
- [63] C. Vidal, J. García-Álvarez, *Green Chem*, 16 (2014) 3515-3521.
- [64] C. Nájera, J. Gil-Moltó, S. Karlström, *Adv Synth Catal*, 346 (2004) 1798-1811.
- [65] K. Kawamura, S. Haneda, Z. Gan, K. Eda, M. Hayashi, *Organometallics*, 27 (2008) 3748-3752.
- [66] M. Trivedi, G. Singh, R. Nagarajan, N.P. Rath, *Inorg Chim Acta*, 394 (2013) 107-116.
- [67] L. Yin, J. Liebscher, *Chem Rev*, 107 (2007) 133-173.

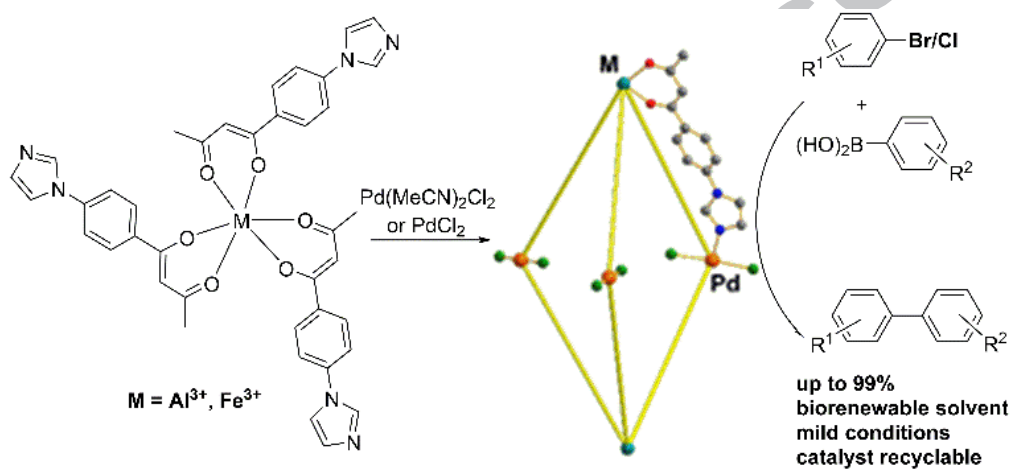
[68] M. Zeng, Y. Du, C. Qi, S. Zuo, X. Li, L. Shao, X.-M. Zhang, *Green Chem*, 13 (2011)

350-356.

[69] K. Mukhopadhyay, B.R. Sarkar, R.V. Chaudhari, *J Am Chem Soc*, 124 (2002) 9692-9693.

### Graphical abstract

Neutral heterometallic  $M_2Pd_3$  supramolecular cages with a trigonal bipyramid geometry have been successfully assembled via the metalloligand strategy on the basis of HSAB theory and exhibit high catalytic activity for the Suzuki–Miyaura coupling reaction in a biorenewable solvent under mild conditions.



### Highlights

- Developed heterogeneous single-site  $M_2Pd_3$  catalyst to prolong catalyst lifetime.
- Highly efficient and recyclable supramolecular catalyst for Suzuki–Miyaura reaction
- Both aryl bromine and aryl chloride were suitable substrates.
- Mild reaction conditions and environment-friendly



ACCEPTED MANUSCRIPT